The ARG algorithm: clinical trials in Argentina

Patricio Colmegna[a,e], **Fabricio Garelli**[b,e], **Hernán De Battista**[b,e], **Fernando Bianchi**[d,e], **Ricardo S. Sánchez-Peña**[c,e]
[a]*University of Virginia, Charlottesville, VA, USA*
[b]*Universidad Nacional de La Plata, Buenos Aires, Argentina*
[c]*Instituto Tecnológico de Buenos Aires, C.A.B.A., Argentina*
[d]*Instituto Balseiro, Comisión Nacional de Energía Atómica, Bariloche, Argentina*
[e]*CONICET, Argentina*

4.1 Introduction

An Artificial Pancreas (AP) is a system to automatically regulate the glucose level in Type 1 Diabetes Mellitus (T1DM), and reduce the constant burden of this disease as much as possible. Although several AP schemes exist [1,2], here we consider that only insulin is infused, and both measurement and infusion are performed subcutaneously via a Continuous Glucose Monitoring (CGM) sensor and an insulin pump. This represents a single-hormone scheme based on a minimally invasive AP system that allows ambulatory use but, unfortunately, makes the control problem much harder.

The main obstacles that have to be taken into account in designing AP controllers are:

- lag-times and errors, both in glucose measurement and insulin action;
- nonlinearities;
- large inter- and intrapatient uncertainties; and
- technical difficulties (sensor dropouts and insulin set failure).

The reader is referred to [3] and [4] for a complete review of these challenges. It is worth remarking that even rapid-acting insulin analogs introduce a significant delay that can affect the performance of a glucose controller [4]. In fact, this is the main limitation for AP systems, considering that the peak of insulin action occurs about 70 min after infusion [5].

The AP development has been accelerated by the use of elaborated simulators (see [6] for a comparison of the most relevant ones). One of them is the UVa/Padova metabolic simulator accepted by the US Food and Drug Administration (FDA) in lieu of animal trials [7,8]. These simulators are instrumental for exhaustive preclinical tests before real-life clinical trials are attempted.

AP clinical trials were performed in different countries of the EU, USA, Israel, and Australia [9–12], and more recently in Argentina [13]. The great majority of the control algorithms that have been clinically tested are based on Proportional-Integral-Derivative (PID), Model Predictive Control (MPC), or fuzzy logic controllers. Generally, they are hybrid (semiautomatic) control loops, where the controller action is complemented with premeal insulin boluses in both single-hormone [14–18] and dual-hormone [2,19] AP schemes. Although the injection of an open-loop bolus based on the carbohydrate intake facilitates the reduction of postprandial glucose values [20], inaccurate carbohydrate counting is frequent [21]. In [2], meal announcement is not required, but it is suggested in order to trigger a meal-priming bolus based on a meal size classification akin to the proposal of [22,23].

Studies involving fully closed-loop AP systems can be found in [24,25] and more recently in [26–29]. Despite promising results, there is still a strong compromise between the aggressiveness of the control action and the postprandial glucose excursion. This compromise exists even when meals can be anticipated based on a probabilistic approach like that presented in [30]. An important aspect to take into consideration when designing glucose controllers is that the counter-regulatory response in people with T1DM is often compromised. Therefore, the response of an AP controller should be designed to be less aggressive than the β-cell's secretory response [4]. However, if the controller is not aggressive enough to a meal perturbation, then prolonged hyperglycemia may occur [20,26]. On the other hand, if the controller is too aggressive, then there is a higher risk of insulin overdosing and, consequently, postprandial hypoglycemia [28]. The latter is partially because the effect of the meal on the CGM signal is not immediate, and therefore the insulin response generated by the controller to cope with the meal is delayed several minutes. It should also be considered that in the standard open-loop basal-bolus treatment, a unique insulin bolus is applied at meal times. Instead, in a feedback control scheme, multiple insulin boluses are generated in response to the change in the CGM signal. As a consequence, fully closed-loop systems have an increased risk of initial hyperglycemia and late hypoglycemia during meals in comparison with semiautomated hybrid strategies. In [29], this problem is reduced, because the insulin bolus to cover the meal is not generated by the multivariable adaptive controller per se, but by an additional module that infuses an insulin bolus when a meal is detected. A very recent set of papers in this area can be found in [31].

In this chapter, a different line of research on control techniques, based on robust and time-varying methods, will be followed [32–35] to overcome the obstacles previously mentioned. In particular, the so-called Automatic Regulation of Glucose (ARG) algorithm will be described. It is based on a switched Linear Quadratic Gaussian (LQG) controller, which works in combination with a sliding-mode safety layer to include Insulin on Board (IOB) constraints [36,37]. To cope with the trade-off between fasting and prandial periods, the switched controller has two modes: one *conservative*, which is active most of the time, and one *aggressive*, which is triggered during meals. The combination of this controller with the safety mechanism allows compensating for delays associated with subcutaneous insulin infusion. When the *ag-*

gressive mode is selected, an insulin spike is generated. This mimics the first-phase insulin secretion of the β-cell response [4]. On the other hand, the purpose of the safety layer is to reduce the insulin infusion commanded by the switched LQG controller when a predefined IOB limit is going to be violated. This latter characteristic can be associated with the suppression of the β-cell in proportion to plasma insulin levels [4]. In this way, an initial "underdamped" insulin response can be generated to compensate for insulin delays, without increasing the risk of postprandial hypoglycemia. It is worth remarking that this is the first time the safety layer is employed to adapt a closed-loop control without premeal insulin boluses.

The proposed control structure also intends to simplify both controller tuning and implementation. This facilitated its in vivo validation in the second phase of the first AP clinical trial campaign in Latin America. There it was tested on five T1DM adults during 36 hours without carbohydrate counting. In the first phase, a hybrid controller was tested in the same site and by the same team [13].

Finally, it should be added that a more demanding regional situation increases the difficulty of this worldwide problem. In Latin America and in developing countries in general, limited budgets and the lack of required personnel is a major obstacle. The high costs in the case of T1DM derived from the frequent, complex, and expensive use of emergency services could be improved by the use of technology in self-management support [38]. In particular, in Argentina for Type 2 Diabetes Mellitus (T2DM), the frequent combination of late diagnosis, inappropriate quality of care, and uneven access to treatment play against the effectiveness and feasibility of secondary prevention. Lack of suitable medication coverage affecting the public health sector also conspires against the provision of effective care [39,40]. In the case of T1DM in Argentina, insulin pumps are available for only 1% of the total amount of T1DM patients (4100 for 400000 patients) from two companies (Roche and Medtronic). Only 15% of the previous pumps are used in a Sensor augmented pump (SAP) fashion (600 patients). The statistics of T1DM over the total number of diabetic patients is similar to the worldwide figures (10%), but the technological penetration is far lower.

4.2 Control-oriented models

The main goal of T1DM simulation models is to provide a blood glucose prediction as close as possible to a real situation to perform reliable preclinical tests. However, this class of models is not generally used for controller synthesis due to its mathematical complexity. Therefore simplifications are usually considered at the controller design phase, because most of the well-established theory of control law design accommodates only simpler dynamics that are usually referred to as *control-oriented* models. Thus, although these models have to represent the underlying dynamics, they are mainly obtained for synthesis purposes and have a much simpler mathematical formulation. In addition, it is worth remarking that the use of complex models for synthesis does not necessarily guarantee a better closed-loop performance [41].

Another aspect to take into account in designing glucose controllers is that most metabolic parameters related to the insulin–glucose system are unidentifiable in practice. Therefore some tuning based on only a small number of easily obtainable patient-specific characteristics is recommended for a safe and effective AP [42]. Consequently, a few works have been focused on such personalization [25,43–46]. This argument also holds from a purely robust control framework: the interpatient variability is so large in this particular problem that there is no chance of obtaining a single controller for all possible patients with a decent performance. Hence the solution is to tune the controller to each patient's clinical characteristics.

Personalizing a model to a particular dynamical system in general, e.g., an engine, is usually performed through an identification process. The drawback here is that this procedure in the case of T1DM patients is very invasive and/or unethical.

One interesting approach to obtain a personalized control-oriented model is to adapt a low-order model structure based on a priori patient information. For example, given the patient's Total Daily Insulin (TDI), an insulin sensitivity factor can be obtained using the 1800 rule (1800/TDI) [47]. From the medical point of view, the 1800 rule indicates the maximum drop in glucose concentration, measured in mg/dl, after a 1 U injection of rapid-acting insulin. Since the work in [48], that rule has been used in several studies, both in silico and in vivo, to tune the gain of a Linear Time Invariant (LTI) model to a particular patient [10,32,33,49,50]. Nevertheless, the 1800 rule is an empirical rule, and it is not indicated at which glucose concentration it works best or is most appropriate. This is important because a patient's insulin sensitivity depends, among other factors (see [51,52]), on the glucose concentration, meaning that an LTI representation of the insulin–glucose system is not enough to totally describe it.

Finally, a good control-oriented model should have a structure that allows well-known, reliable, and numerically robust control synthesis techniques to produce a controller that can be implemented in real time. This control design method should be simple enough to allow real-time implementation, but at the same time, it should have sufficient *dynamical richness* to overcome the obstacles mentioned in the Introduction. According to that, good candidates for an AP controller design are Linear Parameter-Varying (LPV) models or sets of switched LPV (LTI) models.

Several LPV models have been proposed in the past [53–58]. In [53] and [54], the Bergman minimal model [59] was considered and transformed into a quasi-LPV model by an appropriate choice of parameters. In [55–57], the Sorensen compartmental model [60] was linearized at different points, which were defined as the vertexes of an affine-LPV model, which covers the original nonlinear one. This model was used as an uncertainty LTI model set, and an $\mathcal{H}_\infty$ controller was designed to control it; hence the time-varying characteristics were not exploited. Finally, in [58], an LPV approach using the Cambridge model [61] was developed.

The control-oriented LPV model used to design the ARG algorithm was developed by two of the authors in [62,63]. Model identification and tuning were performed using the distribution version of the UVA/Padova metabolic simulator [64, 65]. Without going into greater detail, in [63], a low-order LTI model is proposed,

similar to that in [48], where the input corresponds to the subcutaneous insulin infusion (in pmol/min) and the output to the glucose concentration deviation (in mg/dl):

$$G(s) \quad = \quad k\frac{s+z}{(s+p_1)(s+p_2)(s+p_3)}\mathrm{e}^{-15s}. \tag{4.1}$$

Next, the time-varying behavior of the insulin–glucose dynamics is covered through the construction of an average LPV model. To that end, the parameter p_1 is made to vary with respect to the glucose concentration g, whereas the values of the others are fixed as follows: $z = 0.1501$, $p_2 = 0.0138$, and $p_3 = 0.0143$. The gain parameter k is also time-invariant but is adjusted for each particular patient j according to the 1800 rule. In [62,63], it was detected that the 1800 rule in the UVA/Padova simulator is verified on average starting from an initial glucose concentration of 235 mg/dl. Thus the value of k_j should be such that when the model is excited with 1 U of insulin at 235 mg/dl, the glucose drop matches the 1800 rule. The larger the glucose drop, the more sensitive the patient is to insulin, and the greater is the absolute value of k_j.

In summary, a low-order average LPV model is first proposed and then personalized through a parameter that can easily be obtained. Finally, for each patient j, the following state-space representation affine in the parameter p_1 can be obtained:

$$\begin{aligned} \dot{x}(t) \quad &= \quad A(p_1)x(t) + Bu_\Delta(t), \\ y_\Delta(t) \quad &= \quad Cx(t), \end{aligned} \tag{4.2}$$

with

$$A(p_1) \quad = \quad \begin{bmatrix} 0 & 1 & 0 \\ 0 & 0 & 1 \\ 0 & -p_2p_3 & -(p_2+p_3) \end{bmatrix} + p_1 \begin{bmatrix} 0 & 0 & 0 \\ 0 & 0 & 0 \\ -p_2p_3 & -(p_2+p_3) & -1 \end{bmatrix}, \tag{4.3}$$

$$B \quad = \quad \begin{bmatrix} 0 & 0 & 1 \end{bmatrix}^T, \quad C = k_j \begin{bmatrix} z & 1 & 0 \end{bmatrix}.$$

Since this modeling strategy is intended for controller design, the ν-gap metric (see [66], [67]) is employed to quantify the quality of achievable closed-loop performance afforded by the control-oriented model. In [63], it is shown that this LPV model has a better fit with the simulator in terms of the Root Mean Square Error (RMSE) and also with the ν-gap metric than others presented previously in this area. This fact indicates a potentially better closed-loop performance when designing a controller based on this personalized LPV model.

Additionally, (in)validation results have been produced, which not only verify the effectiveness of the initial (nominal) model presented previously, but also provide a set of models described by the nominal one and a (dynamic) uncertainty bound [69] as follows: $\mathcal{G} = \{G(\rho)[1 + W_\delta(s)\Delta], \Delta \in \mathbb{C}, |\Delta| < \gamma\}$. This framework is adequate for robust controller design methods such as $\mathcal{H}_\infty$ optimal control, LPV, or switched (LTI) LPV control. The theory for model (in)validation has been initially proposed in [70] and can be illustrated through Fig. 4.1. Note that, according to Popper [68],

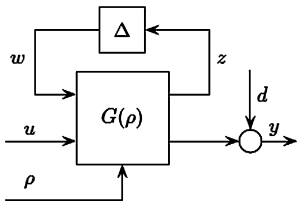

FIGURE 4.1

Identification/invalidation setup.

a theory (or in this case a dynamical model) can only be *falsified* or *invalidated* with certainty, never validated. This is because future data (that might (in)validate the theory) are not accessible. This justifies the use of the term (in)validation.

There an initial LPV model represented by $G(\rho)$, where ρ is a measurable time-varying parameter, is (in)validated against experimental data provided by vectors $[u(t_k), y(t_k), \rho(t_k)]$, $k = 1, \ldots, m$. An optimization problem finds the minimum bounds on the uncertainty $\Delta \in \mathbb{C}$ and the output noise d so that the data streams $[u(t), y(t), \rho(t)]$ could have been produced by this model with noise and uncertainty belonging to the sets inside these bounds. This is defined as consistency, and for these bounds, the model, uncertainty, and noise sets are *not* invalidated by the existing data. The optimization process either fixes one bound and minimizes the other or minimizes a weighted combination of both bounds simultaneously.

Here the idea is to use the LPV model presented previously, define a very small noise bound for d, and determine the minimum uncertainty bound for $|\Delta| < \gamma$ so that this model is consistent with the *experimental* noiseless evidence obtained from the UVA/Padova simulator. This procedure follows the works in [71,72].

Two different inputs have been used to excite all the in silico patients of the distribution version of the UVA/Padova simulator, except for Adult #007. That virtual patient has been excluded from the modeling process and from this analysis, because it has an insulin sensitivity that is not coherent with its TDI. A small bound[1] on the measurement noise $\|d\| < 0.05$ was fixed, and the weight representing the distribution of uncertainty as a function of frequency was $W_\delta(s) = 0.2\frac{500s+1}{50s+1}$. This indicates a 20% uncertainty for frequencies below 2×10^{-3} rad/min, the latter being the maximum achievable closed-loop bandwidth.

The minimum uncertainty bound γ in the model set $\mathcal{G}$ is obtained through optimization. Two different realistic inputs were applied: a 1 U insulin bolus and a modulation of the basal insulin depicted in Fig. 4.2 (left). Both inputs were combined with glucose values of (70, 95, 120, 140, 170, 200) mg/dl. The results that cover both cases at all glucose values are presented in Fig. 4.2 (right). Note that with these results it is possible to personalize each patient's model set. The values of γ lower

[1] $\|\cdot\|$ represents the energy of the signal: $\|d\|^2 = \int_0^\infty |d(t)|^2\, dt$.

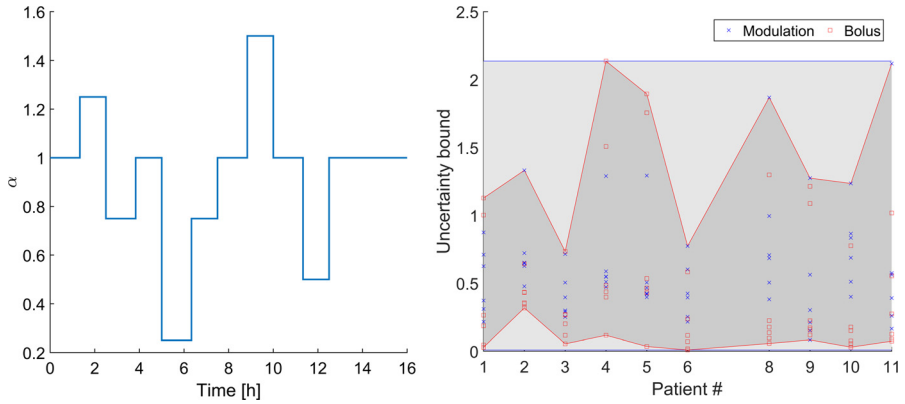

FIGURE 4.2 Invalidation results.

Modulation of basal insulin infusion rate (left) and uncertainty bounds for the in silico patients (right).

(greater) than unity indicate that the uncertainty set should be smaller (larger) than that established initially by W_δ.

4.3 ARG algorithm

For a given subject j, the closed-loop glycemic regulation system with the ARG algorithm is illustrated in Fig. 4.3. As shown in the figure, the algorithm has two main components:

- a switched LQG regulator; and
- a safety layer called SAFE (Safety Auxiliary Feedback Element).

In a first instance and with an introductory purpose, the interaction between these two components will be discussed. Subsequently, each element will be explained with detail.

As it is usual in a closed-loop system, there is a reference signal r, which in this particular case is the desired glucose concentration at fasting state. The difference between the desired glucose concentration and the CGM measurement is defined as the error signal e, which is the input to the ARG algorithm. Since there is no integral action, to avoid insulin stacking, the control signal $u_{\mathcal{C}}$ generated by the switched LQG output is added to the patient's basal insulin infusion rate $i_{b,j}$, thus generating the signal u. If the SAFE block were not present, the signal u would command the insulin pump. However, the presence of the SAFE layer, where u is its input and γ is its output, modulates the proposed infusion rate u to avoid an insulin overdose. In this way, the control action that commands the insulin pump is u_γ, consisting in the infusion rate proposed by the switched LQG regulator multiplied by the output of the

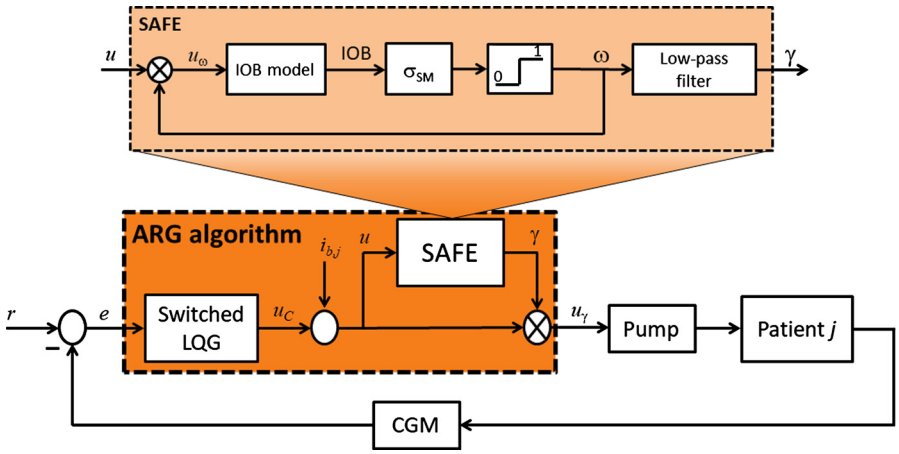

FIGURE 4.3

Closed-loop system with the ARG algorithm.

SAFE block γ. For a more detailed description of the algorithm, the reader is referred to [35].

4.3.1 Switched LQG regulator

Given a patient j, the switched LQG regulator is constituted by two LQG regulators: $\mathcal{K}_{1,j}$ and $\mathcal{K}_{2,j}$. Controller $\mathcal{K}_{1,j}$ makes smooth adjustments on the basal insulin infusion rate, whereas $\mathcal{K}_{2,j}$ is conceived for fast and aggressive corrections. To switch into the *aggressive* mode, the meal can be detected by manually announcing the meal time or by inferring it, for example, from CGM trends. The problem that arises with an automatic mechanism is the strong compromise between a fast detection and immunity to CGM noise. For this reason, a meal announcement was combined with CGM trend observation for controller switching during the first clinical trials with the ARG algorithm, although good in silico results using an automatic mechanism had been obtained previously [32–34,63].

It should be noted that despite announcing the meal time, patients do not have to count the amount of carbohydrates that is about to ingest, translating thus in a lower burden in their daily tasks. Once the meal has been announced, the algorithm does not commute immediately to the *aggressive* controller $\mathcal{K}_{2,j}$, but switches into a *listening* mode in which the CGM signal trend is processed. When a sustained rise in glucose concentration is detected, the commutation to $\mathcal{K}_{2,j}$ is produced with the purpose of generating a control action similar to the standard meal bolus. The commutation from $\mathcal{K}_{2,j}$ back to $\mathcal{K}_{1,j}$ is produced in an automatic manner after 1 hour of operation of the *aggressive* controller, but other strategies involving the SAFE layer could be exploited.

Concerning the design stage, both LQG regulators are designed based on the following model:

$$G_j(s) \quad = \quad k_j \frac{s+z}{(s+p_1^*)(s+p_2)(s+p_3)} \mathrm{e}^{-15s}, \tag{4.4}$$

which is an LTI version of the aforementioned personalized LPV model with $p_1^* = p_1(120)$. The reason for evaluating p_1 at 120 mg/dl is the closed-loop reference, and therefore the glucose value approximately reached without external perturbations.

Since the CGM sensor does not send measures continuously, but rather every 5 min, the continuous-time model $G_j(s)$ is discretized by means of a zero-order hold. Given the following realization of the discrete-transfer function:

$$\begin{aligned} x(k+1) &= A_j x(k) + B_j u_\Delta(k), \\ y_\Delta(k) &= C_j x(k), \end{aligned} \tag{4.5}$$

with $u_\Delta(k) = u(k) - i_{b,j}$ and $y_\Delta(k) = y(k) - 120$ mg/dl, a state feedback control is proposed:

$$u_\Delta(k) \quad = \quad -K_{i,j} x(k), \tag{4.6}$$

which minimizes the following functional cost:

$$J_i(u_\Delta, y_\Delta) \quad = \quad \sum_{k=0}^{\infty} \left(R_i u_\Delta^2 + Q y_\Delta^2 \right) \tag{4.7}$$

with $R_1 = 1$, $R_2 = 0.5$, and $Q = 5 \times 10^3$. The parameter R_2 is defined smaller than R_1 in order $\mathcal{K}_{2,j}(z)$ to be more aggressive than $\mathcal{K}_{1,j}(z)$. In addition, the states are estimated with a Kalman filter of the form

$$\hat{x}(k+1|k) \quad = \quad A_j \hat{x}(k|k-1) + B_j u_\Delta(k) + L_{i,j}[y_\Delta(k) - C_j \hat{x}(k|k-1)], \tag{4.8}$$

where $L_{i,j}$ is obtained assuming that the process noise $w(k)$ and the measurement noise $v(k)$ correspond to white noise satisfying

$$E[w(k)w(k)^T] \quad = \quad W, \quad E[v(k)v(k)^T] = V_i, \tag{4.9}$$

with $W = V_1 = 3$ and $V_2 = 45 \times 10^{-4}$. Here V_2 is defined smaller than V_1 in order $\mathcal{K}_{2,j}(z)$ to have a faster response than $\mathcal{K}_{1,j}(z)$.

Both controllers $\mathcal{K}_{1,j}(z)$ and $\mathcal{K}_{2,j}(z)$ have an observer structure with state feedback and constitute the switched controller. To build a multicontroller, the results presented in [73] have been applied. The details are beyond the scope of this chapter, but the basic idea is to arrange the switched controller into a framework where it can arbitrarily switch between both LQG controllers in a simple manner and without the need to reset the states.

4.3.2 SAFE layer

The SAFE layer, depicted in Fig. 4.3, is based on the sliding-mode reference conditioning technique, developed by one of the authors in his PhD thesis [74]. This technique, designed in general for control of constrained systems, was first applied in T1DM in [36] and then successfully tested on clinical trials in Spain. Its main objective is to modulate the gain of the controller to prevent IOB from stacking by imposing a constraint $\overline{\text{IOB}}(t)$. Thus this layer helps to minimize the risk of hypoglycemia in late postprandial periods.

The core element of any sliding-mode control is the switching logic, which in this case is

$$w(t) = \begin{cases} 1 & \text{if } \sigma_{\text{SM}}(t) > 0, \\ 0 & \text{else,} \end{cases} \tag{4.10}$$

where $\sigma_{\text{SM}}(t)$ is the sliding function defined simply as the difference between the actual IOB level and the imposed personalized limit:

$$\sigma_{\text{SM}}(t) = \overline{\text{IOB}}_j(t) - \text{IOB}(t). \tag{4.11}$$

The limit $\overline{\text{IOB}}_j(t)$ is a priori considered piecewise constant, as it is explained later.

Because IOB cannot be measured in real time, it must be estimated. To this effect, the model presented in [75] is considered:

$$\begin{aligned} \dot{I}_{sc1}(t) &= -K_{\text{DIA}} I_{sc1}(t) + u_w(t), \\ \dot{I}_{sc2}(t) &= K_{\text{DIA}} \left[I_{sc1}(t) - I_{sc2}(t) \right], \\ \text{IOB}(t) &= I_{sc1}(t) + I_{sc2}(t), \end{aligned} \tag{4.12}$$

where I_{sc1} and I_{sc2} are, respectively, the amount of nonmonomeric and monomeric insulin in the subcutaneous space, u_w is the exogenous insulin infusion rate in pmol/min/kg, and K_{DIA} [min^{-1}] is a constant rate. The advantage of this model is that it can be easily customized via K_{DIA} so as to replicate each patient's duration of insulin action (DIA) [47]. It should be noted that DIA is a clinical parameter adjusted in commercial insulin pumps. As a starting point, an average DIA of 5 hours was selected, leading to a K_{DIA} fixed at 16.3×10^{-3} min^{-1} [37].

When the $\overline{\text{IOB}}_j(t)$ limit is reached by the IOB estimation, a sliding regime is established over the surface $\sigma_{\text{SM}}(t) = 0$. During this mode, from (4.10), the signal $w(t)$ switches at high frequency between 0 and 1 to fulfill the imposed restriction and forces system (4.12) to remain within the invariant set

$$\Sigma = \{x(t) \mid \sigma_{\text{SM}}(t) \geq 0\}, \tag{4.13}$$

where $x(t) \in \mathbb{R}^2$ are the states of (4.12). The switching signal $w(t)$ is then smoothed by a first-order filter (or averaged between infusion intervals), giving place to $\gamma(t)$, which is the factor that finally modulates the signal commanding the pump.

Observation: It is easy to prove that the derivative of the switching function $\sigma_{\text{SM}}(t)$ depends on the control action $u_w(t)$ and therefore on the discontinuous action $w(t)$, which is a necessary condition for establishing the sliding mode, known as transversality condition.

Like the main controller, the SAFE layer is implemented in a discrete way, obtained from (4.12) as follows:

$$\begin{aligned} x(k+1) &= \begin{bmatrix} 1 - K_{\text{DIA}} T_r & 0 \\ K_{\text{DIA}} T_r & 1 - K_{\text{DIA}} T_r \end{bmatrix} x(k) + \begin{bmatrix} 1 \\ 0 \end{bmatrix} u_w(k), \\ \text{IOB}(k) &= \begin{bmatrix} 1 & 1 \end{bmatrix} x(k), \end{aligned} \tag{4.14}$$

where $T_r = 0.1$ min is the selected sample time. It should be noticed that T_r is smaller than $T_s = 5$ min since the SAFE algorithm is programmed entirely in software, and thus the switching frequency is only limited by the speed of the platform's microprocessor.

Although there may be different criteria to define the IOB limit, in this first approach, the following classification of the meal size was defined:

- Small meal < 35 gCHO. $\overline{\text{IOB}}_{\text{s},j}(t) = \text{IOB}_{\text{ss},j}(t) + 40$ gCHO/$\text{CR}_j(t)$.
- Medium meal $[35, 65)$ gCHO. $\overline{\text{IOB}}_{\text{m},j}(t) = \text{IOB}_{\text{ss},j}(t) + 55$ gCHO/$\text{CR}_j(t)$.
- Large meal ≥ 65 gCHO. $\overline{\text{IOB}}_{\text{l},j}(t) = \text{IOB}_{\text{ss},j}(t) + 70$ gCHO/$\text{CR}_j(t)$.

Here $\text{IOB}_{\text{ss},j}(t)$ is the steady-state value of model (4.14) corresponding to the patient's basal insulin rate $i_{b,j}(t)$, and X gCHO/$\text{CR}_j(t)$ is the insulin bolus related to X grams of carbohydrates (gCHO) using the patient's Carbohydrate Ratio (CR) in [g/U]. When the system is not at a prandial period, the IOB limit is fixed to $\overline{\text{IOB}}_{\text{s},j}(t)$. In this manner, the controller has an extra degree of freedom to make adjustments to the basal infusion rate when necessary.

4.3.3 Auxiliary modules

To minimize the risks of hypo- and hyperglycemia, two auxiliary modules, which are discussed below, have been added to the ARG algorithm to make it more robust against the time-varying nature and high uncertainty of the insulin–glucose dynamics.

Hypoglycemia-related module (Hypo-RM)

Here an algorithm to lower the IOB limit when low glucose values are detected or predicted is defined as follows.

1: At every sampling time:
2: The glucose measured by the CGM sensor (g) in mg/dl is received, and a linear extrapolation strategy is used to estimate the glucose rate of change ($\hat{\dot{g}}_{30}$) in mg/dl/min. Besides, the future glucose concentration is predicted with a forecasting horizon of 15 min ($\hat{g}_{15}$), considering the last six glucose measurements, that is, the CGM samples received during the last 30 min.

3: The IOB limit is set according to previous sections.
4: **if** $g < 60$ **then**
5: $\quad \overline{\text{IOB}}_j(t) = 0$
6: **else if** $g < 70$ **then**
7: $\quad \overline{\text{IOB}}_j(t) = 0.5\text{IOB}_{\text{ss},j}(t)$
8: **else if** $i = 1$ **and** $\ell = 0$ **then**
9: $\quad$ **if** $\hat{\dot{g}}_{30} < -0.5$ **or** $[\hat{\dot{g}}_{30} < 0.5$ **and** $\text{IOB}(t) \geq \text{IOB}_{\text{ss},j}(t)]$ **then**
10: $\quad\quad$ **if** $\hat{g}_{15}$<70 **then**
11: $\quad\quad\quad \overline{\text{IOB}}_j(t) = 0.5\text{IOB}_{\text{ss},j}(t)$
12: $\quad\quad$ **else if** $\hat{g}_{15}$<100 **then**
13: $\quad\quad\quad \overline{\text{IOB}}_j(t) = 0.75\text{IOB}_{\text{ss},j}(t)$
14: $\quad\quad$ **else if** $\hat{g}_{15}$<120 **then**
15: $\quad\quad\quad \overline{\text{IOB}}_j(t) = \text{IOB}_{\text{ss},j}(t)$
16: $\quad\quad$ **end if**
17: $\quad$ **end if**
18: **end if**

In this way, the Hypo-RM module has the following levels of action:

- **Level A**: $\overline{\text{IOB}}(t) = 0$.
- **Level B**: $\overline{\text{IOB}}(t) = 0.5\text{IOB}_{\text{ss}}(t)$.
- **Level C**: $\overline{\text{IOB}}(t) = 0.75\text{IOB}_{\text{ss}}(t)$.
- **Level D**: $\overline{\text{IOB}}(t) = \text{IOB}_{\text{ss}}(t)$.

In addition, note that the code below Line 8 is executed only if the controller is in conservative mode ($i = 1$) and in non*listening* mode ($\ell = 0$).

Hyperglycemia-related module (Hyper-RM)

This module generates a Correction Bolus (CB) in [U] based on the patient's Correction Factor (CF) in [U/mg/dl] when a persistent hyperglycemic excursion cannot be mitigated by the conservative mode of the ARG algorithm.

1: At every sampling time:
2: A Boolean variable HYPOFLAG is set to unity if the Hypo-RM was activated and to zero otherwise.
3: The glucose rate of change ($\hat{\dot{g}}_{30}$) and the future glucose concentration ($\hat{g}_{15}$) determined in the Hypo-RM are considered here, together with the glucose rate of change estimated from the last three CGM samples ($\hat{\dot{g}}_{15}$).
4: The mean value of the last six CGM samples ($\overline{g}_{30}$) is calculated.
5: A Boolean variable G160FLAG, which is zero by default, is set to unity if the last six CGM samples are higher than 160 mg/dl.
6: Timers CCBOLUS and CAGGCON that count the minutes elapsed from the last CB and from the last aggressive–conservative commutation are updated.
7: **if** $i = 1$ **and** $\ell = 0$ **then**
8: $\quad$ **if** HYPOFLAG=0 **and** CCBOLUS$\geq$ 120 **and** CAGGCON$\geq$ 180 **then**
9: $\quad\quad$ **if** (G160FLAG=1 **and** $\hat{\dot{g}}_{30} \geq 0$ **and** $\hat{\dot{g}}_{15} \geq -0.5$) **or** $\overline{g}_{30} > 200$ **then**
10: $\quad\quad\quad$ CB = $0.8[\min(\overline{g}_{30}, \hat{g}_{15})\text{-}120]/\text{CF}$

11: **end if**
12: **end if**
13: **end if**

Note that according to the conditions that have to be fulfilled for the generation of a CB, this module is likely to be activated only during fasting periods of persistent hyperglycemia. The minimum between $\overline{g}_{30}$ and $\hat{g}_{15}$ and the 0.8 factor are considered to be conservative, because the measurement noise could lead to overestimate the value of the CB. In addition, for safety, the CB is not directly infused to the patient. Instead, it is added to the insulin bolus proposed by the ARG algorithm to avoid violating the IOB limit.

4.4 Simulations

All the in silico experiments were carried out with the UVA/Padova simulator considering:

- a Dexcom G4 Share CGM;
- a generic insulin pump with a quantization of 0.1 U and a maximum bolus of 25 U (these characteristics are analogous to Roche Accu-Check Combo pump);

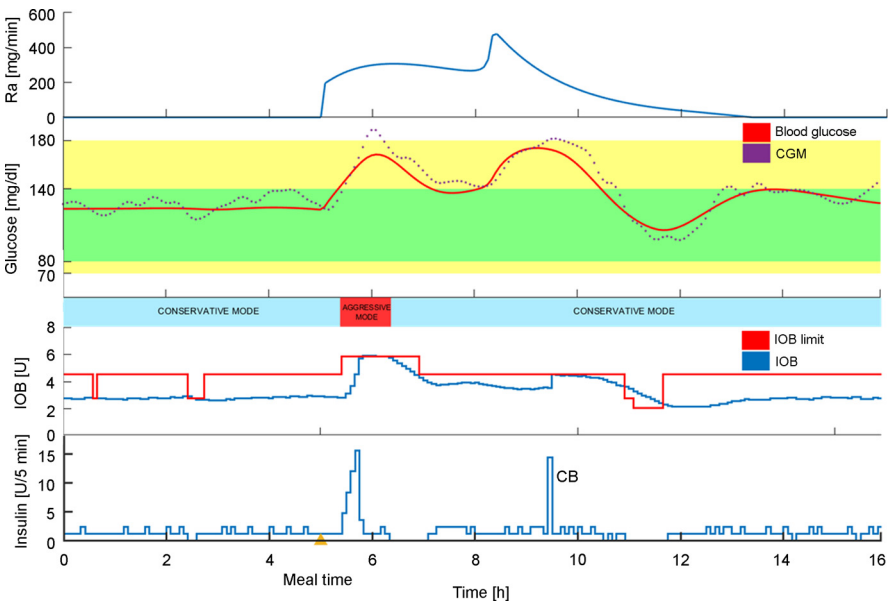

FIGURE 4.4 How the ARG algorithm works.

Closed-loop response for an in silico adult of the UVA/Padova simulator when a mixed meal is ingested. The meal intake happens 5 hours after the beginning of the simulation.

- a glucose reference of 120 mg/dl; and
- meal time announcement.

Fig. 4.4 shows how the ARG algorithm works. In that figure, the response to a mixed meal (milk, white bread, low-fat cheese, butter, oil; CHO = 111.0 g) from the meal library presented in [76] is depicted. Note that the glucose rate of appearance (R_a) associated with this meal has two peak values: one at meal time and the other one around 3 hours later. The controller $\mathcal{K}_1$ was in charge of the insulin infusion most of the time, whereas $\mathcal{K}_2$ only worked during the prandial period. Once the controller $\mathcal{K}_2$ was selected, larger insulin boluses were delivered to avoid postprandial hyperglycemia. These boluses were modulated by the SAFE layer through the signal γ to avoid the violation of the imposed constraint on the IOB. In this way, excessive insulin stacking was avoided, and the risk of hypoglycemia was reduced. From this analysis it can be seen that while the aggressive controller ($\mathcal{K}_2$) diminishes hyperglycemia, the SAFE protection avoids hypoglycemia. Both systems work together in such a way to maintain the patient glycemia in the desirable [70, 180] mg/dl or acceptable [70, 250] mg/dl range. Finally, Fig. 4.4 also illustrates how both auxiliary modules assist in regulating the glucose level. The Hypo-RM lowers the IOB limit when hypoglycemic situations are predicted, whereas the Hyper-RM generates CBs to complement the action of the conservative controller when necessary. In this case, a CB was generated because the late second peak in R_a could not be completely mitigated by the conservative controller $\mathcal{K}_1$.

Another important aspect to point out is that the peak in the insulin infusion happens after the meal intake, opposed to the traditional therapy where the meal bolus is ideally delivered minutes before eating. This delay is due to the feedback strategy. Here the effect of the meal on the glucose level is not detected by the CGM until some minutes after the intake. This results in an inevitable increase in glucose concentration, which is later compensated by the aggressive LQG controller. Other control strategies have a hybrid structure, in which a feedforward meal bolus is injected at meal times and the controller is only in charge of regulating the basal delivery rate. In this way, postprandial peaks could be reduced as the bolus would be infused at an earlier time than with the proposed strategy. Nonetheless, the patient would be responsible of carbohydrate counting, which is rarely exact in daily life and also imposes a task that goes against his/her quality of life.

Fig. 4.5 depicts the average closed-loop responses and the Control Variability Grid Analysis (CVGA) plot for all the in silico adults of the complete UVA/Padova simulator to meals of 25, 50, and 75 gCHO. In all cases, a medium-meal IOB limit, that is, $\overline{\text{IOB}}_j(t) = \overline{\text{IOB}}_{\text{m},j}(t)$, was set to test the robustness of the ARG algorithm to errors in meal size classification.

The different regions of the CVGA represent glycemic control as follows: A-zone, accurate control; lower and upper B-zones, benign deviations into hypo- and hyperglycemia; B-zone, benign control deviations; upper and lower C-zone, overcorrection of hypo- and hyperglycemia; lower and upper D-zone, failure to deal with hypo- and hyperglycemia; and E-zone, erroneous control. As previously mentioned, since a feedforward insulin bolus is not injected at meal times, the upper B-zone has

Table 4.1 In silico closed-loop data. In silico closed-loop results with the ARG algorithm. The overall (O) and the postprandial period (PP) defined previously are analyzed separately.

		25 gCHO meal			50 gCHO meal			75 gCHO meal		
		Mean	**Median**	**IQR**	**Mean**	**Median**	**IQR**	**Mean**	**Median**	**IQR**
Blood Glucose [mg/dl]	**O**	127	126	[121, 131]	134	133	[128, 137]	143	142	[136, 148]
	PP	135	133	[126, 141]	160	159	[150, 167]	188	186	[175, 196]
% time in [70, 250] mg/dl	**O**	99.7	100	[100, 100]	99.6	100	[100, 100]	96.7	100	[94.8, 100]
	PP	99.4	100	[100, 100]	99.0	100	[100, 100]	89.7	100	[83.3, 100]
% time in [70, 180] mg/dl	**O**	98.7	100	[100, 100]	89.8	90.9	[88.1, 92.2]	83.0	83.8	[80.6, 86.8]
	PP	96.3	100	[100, 100]	67.7	71.0	[62.0, 75.0]	46.4	48.0	[38.0, 57.8]
% time $>$ 250 mg/dl	**O**	0.0	0.0	[0.0, 0.0]	0.3	0.0	[0.0, 0.0]	3.2	0.0	[0.0, 5.2]
	PP	0.0	0.0	[0.0, 0.0]	0.9	0.0	[0.0, 0.0]	10.3	0.0	[0.0, 16.8]
% time $>$ 180 mg/dl	**O**	1.0	0.0	[0.0, 0.0]	10.1	9.1	[7.8, 11.8]	16.9	16.3	[13.2, 19.4]
	PP	3.1	0.0	[0.0, 0.0]	32.2	29.0	[25.0, 38.0]	53.6	52.0	[42.3, 62.0]
% time $<$ 70 mg/dl	**O**	0.3	0.0	[0.0, 0.0]	0.1	0.0	[0.0, 0.0]	0.1	0.0	[0.0, 0.0]
	PP	0.6	0.0	[0.0, 0.0]	0.1	0.0	[0.0, 0.0]	0.0	0.0	[0.0, 0.0]
% time $<$ 50 mg/dl	**O**	0.0	0.0	[0.0, 0.0]	0.0	0.0	[0.0, 0.0]	0.0	0.0	[0.0, 0.0]
	PP	0.1	0.0	[0.0, 0.0]	0.0	0.0	[0.0, 0.0]	0.0	0.0	[0.0, 0.0]
LBGI		0.1	0.0	[0.0, 0.1]	0.1	0.0	[0.0, 0.0]	0.0	0.0	[0.0, 0.1]
HBGI		0.9	0.8	[0.6, 1.2]	2.0	1.8	[1.5, 2.3]	3.6	3.3	[2.7, 4.0]

IQR, interquartile range.

a larger density of points. However, this does not imply a greater risk to the patients' health. In addition, the fact that a few subjects are in the C (2.7%), D (1.3%), and E (0.3%) zones could be analyzed as follows. On one hand, it must be considered that not every in silico patient has parameters that make sense physiologically, given that the database was generated for statistical ends. On the other hand, the proposed strategy allows tackling the singular cases where the controller action was either too conservative or too aggressive by slightly regulating the IOB constraint in terms of postprandial hypo- or hyperglycemia frequency.

Numerical outcomes for all the considered cases are presented in Table 4.1. There the closed-loop results obtained in both the overall (O) and the 5-hour time interval following the start of the meal (postprandial period, PP) are analyzed separately. The Low Blood Glucose Index (LBGI) and the High Blood Glucose Index (HBGI) are also included. The scale for these indexes are defined according to [77]:

- **Risk of hypoglycemia:** LBGI ≤ 2.5 (low); $2.5 <$ LBGI ≤ 5 (moderate); LBGI > 5 (high).
- **Risk of hyperglycemia:** HBGI ≤ 4.5 (low); $4.5 <$ HBGI ≤ 9 (moderate); HBGI > 9 (high).

We can observe that the ARG algorithm allowed achieving minimal risk of hypo- and hyperglycemia. Even though the results are satisfactory, they can be further improved with the addition of the aforementioned meal size classifier to help establish a more adequate IOB constraint. For example, when the small-meal IOB limit $\overline{\text{IOB}}_{\text{s},j}$ is used in the simulations with the 25 gCHO meal, the mean time in hypoglycemia is reduced from 0.5% to 0.2%, maintaining a mean time of 96.5% in the range

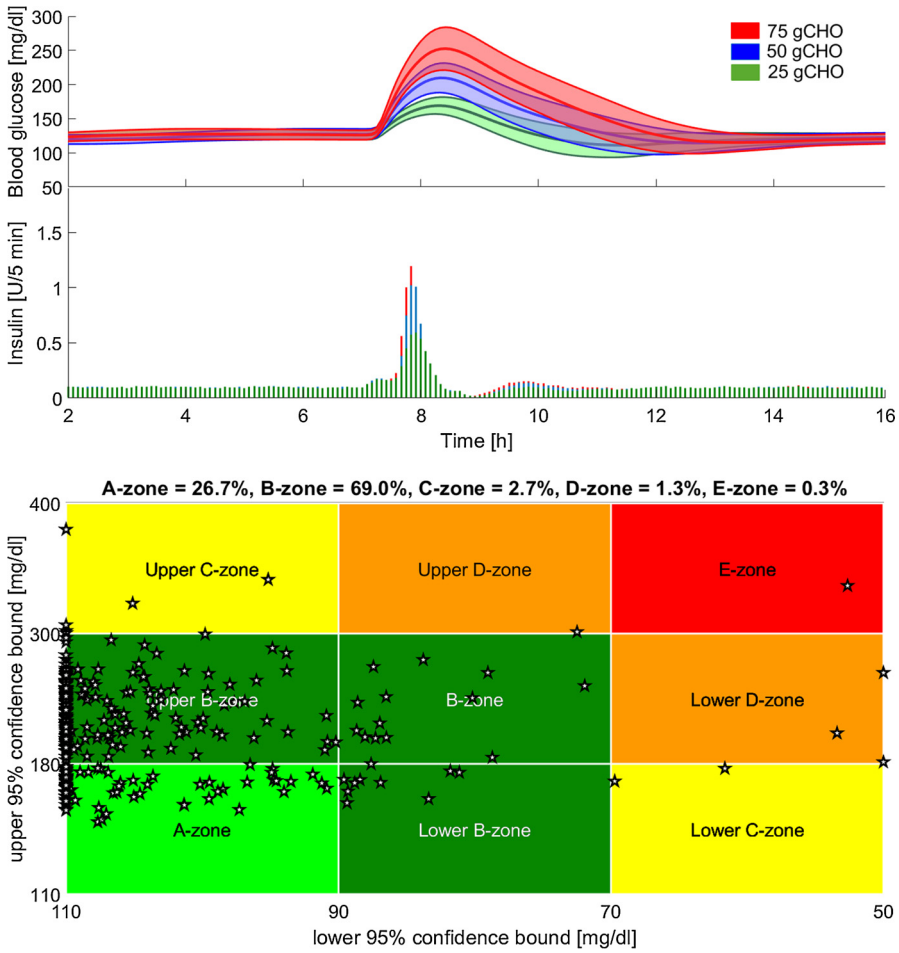

FIGURE 4.5 In silico closed-loop responses.

Upper top: Closed-loop responses for all the in silico adults of the complete UVA/Padova simulator to 25, 50, and 75 gCHO meals. The solid lines indicate the mean glucose, and the shaded areas are ± 1 standard deviations. **Bottom top:** Mean insulin infusions. **Bottom:** CVGA plot.

[70, 180] mg/dl in the postprandial period. On the other hand, when the large-meal IOB limit $\overline{\text{IOB}}_{l,j}$ is used in the simulations with the 75 gCHO meal, the mean time in the range [70, 180] mg/dl increases from 46.3% to 52.5% during the postprandial period, with a minimal increase in the mean time in hypoglycemia from 0.0 to 0.1%.

To further test the performance of the ARG algorithm, simulations considering different initial glucose values and errors in the adjustment of the basal insulin infusion rate were performed with the adult cohort of the distribution version of the

UVA/Padova simulator. Two examples are illustrated in Fig. 4.6. In one case, a high initial glucose concentration of 210 mg/dl along with an insulin infusion rate that leads to a low steady-state glucose value of 70 mg/dl is considered (case 1). In the other case, the opposite scenario is tested, that is, a low initial glucose concentration of 70 mg/dl along with an insulin infusion rate that leads to a high steady-state glucose value of 210 mg/dl (case 2). As shown in the figure, the ARG algorithm was able to safely regulate the glucose level in both cases independently of the conditions. Indeed, the mean time in the range [70, 180] mg/dl was 91.1% for case 1 and 77.1% for case 2, whereas it is 90.0% when considering 120 mg/dl as initial and steady-state glucose value.

4.5 Clinical trials

The first clinical trials with an AP in Latin America were carried out in two stages at the Hospital Italiano de Buenos Aires (HIBA). The first one was in November 2016 with the algorithm of the University of Virginia that had been tested internationally in several occasions. The second trial was in June 2017 with the ARG algorithm, fully developed in Argentina, in collaboration between researchers from the Instituto Tecnológico de Buenos Aires (ITBA), the Universidad Nacional de Quilmes (UNQ), and the Universidad Nacional de La Plata (UNLP). Both stages had the same numbers of patients (5) and hardware and followed the same clinical protocol. However, the

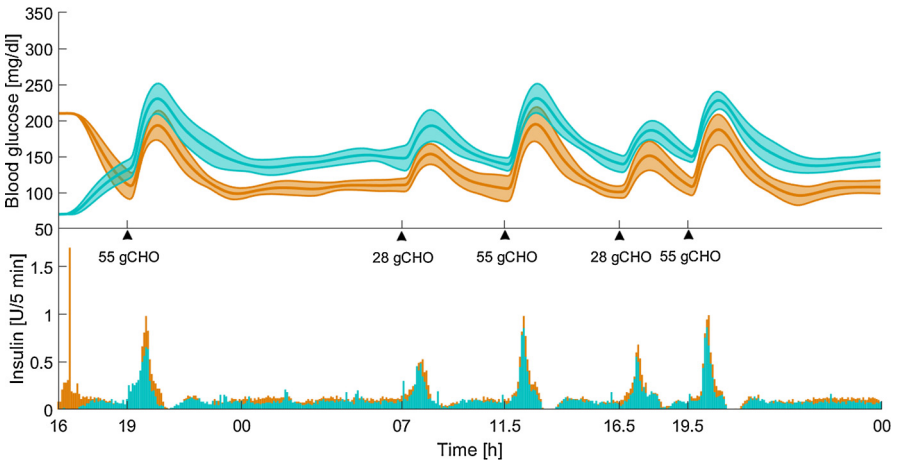

FIGURE 4.6 ***In silico*** **closed-loop responses.**

Above: Closed-loop responses for all the in silico adults of the distribution version of UVA/Padova simulator to different glucose initial conditions and basal insulin rate adjustments. The solid lines indicate the mean glucose, and the shaded areas are ±1 standard deviations. **Below:** Mean insulin infusions.

main difference between both trials is that in the latter, the patients had neither to count CHO nor to apply an insulin bolus. Here we focus on this second clinical trial.

The selection of five patients with T1DM that participated in the trials was made according to the clinical protocol, particularly the inclusion and exclusion criteria as indicated in NCT02994277 (www.clinicaltrials.gov).

4.5.1 Hardware and software

For the implementation of the AP, the following devices were used in each patient:

- CGM Dexcom G4 Share;
- Accu-Check Combo insulin pump from Roche; and
- a NEXUS-5 smartphone based on Android containing the Diabetes Assistant (DiAs) from the University of Virginia (UVa) [78].

The Diabetes Assistant (DiAs) is a software that includes several mobile applications and allows every 5 minutes the communication between the control algorithm, the CGM sensor (through Android Bluetooth Low Energy), and the insulin pump (through standard Bluetooth). Due to FDA regulations, to be accepted as a Class III medical device, the phone, navigator, Android Market, games, and so on were removed. The system also includes the SQLite database for the asynchronous data management for requests from the user.

The DiAs is a modular system where the control algorithm is contained. The ARG algorithm was programmed in the DiAs using object-oriented programming on the Eclipse IDE for Java Developers version: Kepler Service Release 2, with the plugin Android Development Tools (ADT).

4.5.2 Clinical procedures

Patients were called to attend the HIBA nine days before the trial. That day, the protocol was explained in detail, the Informed Consent was signed, the inclusion/exclusion criteria were revised, and a blood extraction was made for laboratory *screening*. These results and a supervised glycaemia control were reviewed two days before the trial. That same day, the insulin pump and the CGM were connected to each patient, with a brief training in the use of both devices. The communication among these devices with the smartphone was verified, and the systems remained in open loop (without the algorithm active in the smartphone) in order for the patients to perform their usual controls. For comparison purposes, they also had to perform eight daily capillary glycaemia measurements until the day of the trial.

The trial started at 1700 hs on day 0 and ended the morning of day 2. The loop was closed by activating the control algorithm in the smartphone, and all patients had five meals during the 36 hs tests: two dinners, one lunch, one breakfast, and one afternoon snack with a continuous monitoring of their glycaemia and injected insulin values from the medical and researcher staff room.

The menu was coordinated by the nutritionist and had the following contents of CHO: breakfast or afternoon snack 28 g (wholegrain bread, water crackers, diet jam, spread cheese with tea, coffee or mate); dinner or lunch 55 g (wheat pasta with natural filetto sauce and lean meat with smashed potatoes, in both cases with fresh fruit).

4.5.3 Results

Table 4.2 Clinical trial data. Comparison of the statistical data obtained from 36 hs in UC vs CL, considering a confidence interval of 95%.

	UC		CL	
	Mean	**CI 95%**	**Mean**	**CI 95%**
% time [70, 250] mg/dl	82.9	[67.3, 98.6]	88.6	[82.4, 94.7]
% time [70, 180] mg/dl	59.1	[41.9, 76.2]	74.7	[68.1, 81.4]
% time $<$ 70 mg/dl	7.6	[2.9, 12.4]	5.8	[1.6, 10.0]
% time $<$ 50 mg/dl	1.7	[0.3, 3.1]	0.8	[0.2, 3.5]
LBGI	2.8	[1.8 3.7]	2.3	[1.4, 3.1]
HBGI	7.2	[3.4, 11.0]	4.9	[2.9, 6.9]

Next, a brief description of the results is presented. The Usual Care (UC) analysis was considered from 7 p.m. on the 21/09 up to 7 a.m. on the 23/09. In the case of the Closed Loop (CL) period, the time interval was considered from 7 p.m. on the 23/09 up to 7 a.m. on the 25/09. The insulin pump of one of the patients had an occlusion during the first night in CL, and therefore these hours were not considered in the analysis. The UC is used as a reference of their habitual glucose management, and it should be noted that the patients did not follow strictly the same diet during UC and CL. In Table 4.2 we can see the statistical data obtained from the 36 hours of CL trial and the comparison with those obtained in UC. We can observe that there is a significant improvement in the patient's glucose regulation when using the ARG algorithm. The null hypothesis at a level of significance of 5% ($\rho = 0.05$), defined as the difference between the results obtained in UC and CL have zero mean, can be rejected in the percentage of time in euglycemic range $[70, 180]$ mg/dl, being statistically significant ($\rho = 0.0356$).

Since this is the first clinical trial of the ARG algorithm, three initial meals were used to make the necessary adjustments to the IOB maximum limit. For this reason, if the analysis of the results is concentrated in the last 15 hours of CL and it is compared with the 15 hours of UC that involve the same period of the day, then an even more significant control improvement is noticed, as it is shown in Table 4.3. The null hypothesis at a level of significance of 5% ($\rho = 0.05$), defined as the difference between the results obtained in UC and CL have zero mean, can be rejected in percentage time in euglycemic range $[70, 180]$ mg/dl ($\rho = 0.0142$), in < 70 mg/dl ($\rho = 0.049$), LBGI index (p $= 0.0383$), and HBGI index ($\rho = 0.0469$), these being statistically significant.

Table 4.3 Clinical trial data. Comparison of the statistical data obtained from first 15 hs in UC and the last 15 hs in CL with a confidence interval of 95%.

	UC		CL	
	Mean	**CI 95%**	**Mean**	**CI 95%**
% time [70, 250] mg/dl	73.5	[49.8, 97.2]	94.7	[83.8, 98.4]
% time [70, 180] mg/dl	49.8	[24.5, 75.1]	82.6	[69.9, 95.2]
% time $<$ 70 mg/dl	13.6	[4.4, 22.7]	4.1	[0.8, 18.0]
% time $<$ 50 mg/dl	5.4	[1.6, 16.4]	0.2	[0.0, 3.5]
LBGI	4.2	[2.1 6.2]	1.8	[0.3, 3.3]
HBGI	8.7	[2.9, 14.5]	2.8	[0.1, 5.5]

It is important to remark that taking into account the night period (from 23 p.m. until 7 a.m.), the ARG algorithm presents a notorious improvement in comparison with the UC treatment. In Fig. 4.7, it is highlighted the comparison of the glucose excursion obtained during the second night in UC and in CL (time lapse without meals). In Table 4.4 the statistical data is presented regarding this period. Again, an improvement in percentage of time in euglycemia ($\rho = 0.0351$) and HBGI index ($\rho = 0.0309$) was obtained. Finally, in Fig. 4.8, the UC and CL percentage time in each glucose range and time-in-range cumulative plots are compared for both overall (36 h trial) and second night periods, showing again the effectiveness of the ARG algorithm.

Table 4.4 Clinical trial data. Comparison of the statistical data obtained from the last nights in UC vs CL with a confidence interval of 95%.

	UC		CL	
	Mean	**CI 95%**	**Mean**	**CI 95%**
% time [70, 250] mg/dl	78.1	[29.1, 96.9]	95	[66.9, 99.4]
% time [70, 180] mg/dl	50.3	[23.2, 77.4]	87.7	[76.5, 99.0]
% time $<$ 70 mg/dl	3.6	[0.3, 29.5]	5	[0.6, 33.1]
% time $<$ 50 mg/dl	0	[0.0, 0.0]	0	[0.0, 0.0]
LBGI	2.0	[0.6, 3.4]	1.5	[0.4, 4.1]
HBGI	9.8	[2.8, 16.8]	1.9	[0.4, 5.7]

4.6 Conclusions

In this chapter, a brief review of the AP project in Argentina was presented alongside with a novel control strategy for glycemic regulation, the ARG algorithm. It consists of a two-degree-of-freedom control structure that includes a switched LQG inner controller together with an outer sliding-mode safety loop, the Safety Auxiliary Feedback Element (SAFE) mechanism, for IOB constraints. The switched LQG

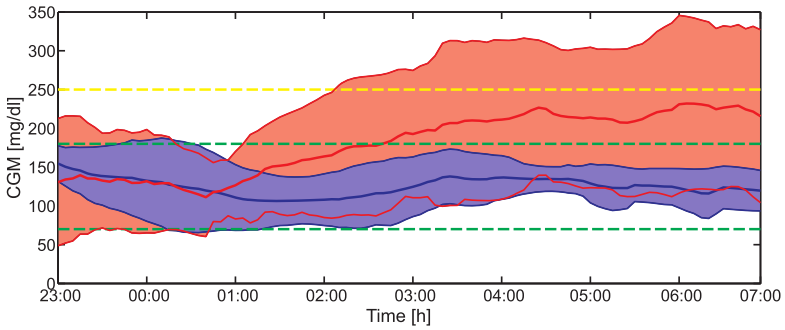

FIGURE 4.7 Clinical test.

Mean glycemic excursion of all five patients in UC (red (mid gray in print version)) and in CL (blue (dark gray in print version)) during night time. The solid line indicates mean, and the gray area ±1 standard deviation.

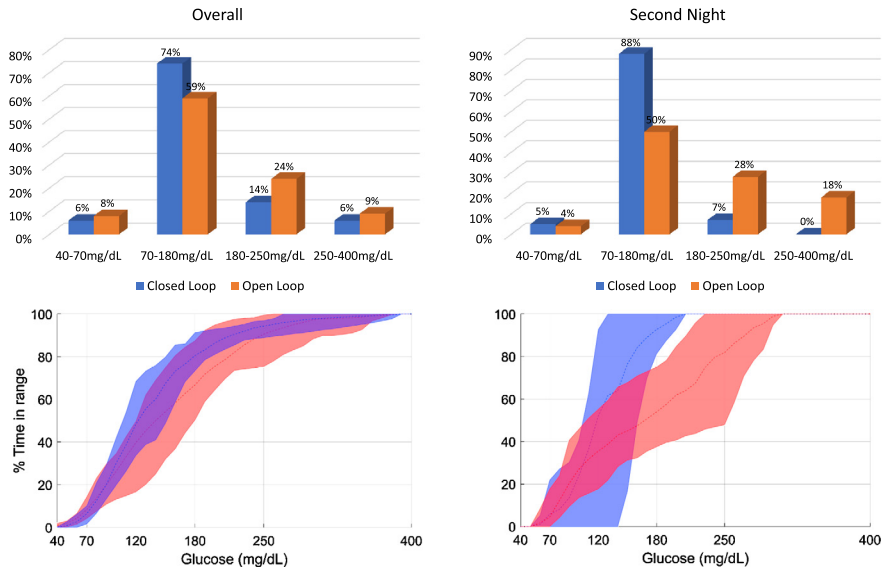

FIGURE 4.8 Clinical test.

Glucose range percentage times and cumulative time-in-range for all patients in UC (red (mid gray in print version)) and in CL (blue (dark gray in print version)) during the whole trial (left half) and during the second night (right half). The dashed lines are the mean values, and the continuous lines are the envelopes.

control strategy is a simplified version of that in [33]. The switched nature of the inner controller enables different tunings for dealing with prandial and fasting periods and can be extended to other situations, for example, physical activity. New and more complex scenarios could be potentially addressed by redesigning the switching

policy and/or the IOB constraints. The SAFE layer quickly adapts the controller gain to automatically obtain insulin spikes like the open-loop boluses. Promising results were obtained both in silico and later in vivo during the first clinical trials in Latin America.

Acknowledgments

Access to the complete version of the University of Virginia/Padova metabolic simulator was provided by an agreement with Prof. C. Cobelli (University of Padova) and Prof. B. P. Kovatchev (University of Virginia) for research purposes. The authors would like to acknowledge Dr. Daniel Cherñavvsky for his very generous collaboration. We would also like to thank the physicians of the Hospital Italiano Ventura Simonovich, Paula Scibona, Cintia Rodriguez, Javier Giunta, and Valeria Beruto coordinated by Dr. Luis Grosembacher and Dr. Waldo Belloso, without whom the clinical trial could not have been possible. Additionally, we express our gratitude to the nutritionist Marianela Stasi, who worked with us in the elaboration of the menu used. The invaluable help during the tests of our students Emilia Fushimi, Marcela Moscoso-Vázquez, and Nicolás Rosales is deeply appreciated. Finally, we want to highlight the collaboration with Dexcom, the generous donation by Roche, and the funding of the Cellex (Spain) and Nuria (Argentina) Foundations.

References

[1] E. Renard, Insulin delivery route for the artificial pancreas: subcutaneous, intraperitoneal, or intravenous pros and cons, J. Diabetes Sci. Technol. 2 (4) (2008) 735–738.

[2] F.H. El-Khatib, C. Balliro, M.A. Hillard, K.L. Magyar, L. Ekhlaspour, M. Sinha, D. Mondesir, A. Esmaeili, C. Hartigan, M.J. Thompson, S. Malkani, J.P. Lock, D.M. Harlan, P. Clinton, E. Frank, D.M. Wilson, D. DeSalvo, L. Norlander, T. Ly, B.A. Buckingham, J. Diner, M. Dezube, L.A. Young, A. Goley, M.S. Kirkman, J.B. Buse, H. Zheng, R.R. Selagamsetty, E.R. Damiano, S.J. Russell, Home use of a bihormonal bionic pancreas versus insulin pump therapy in adults with type 1 diabetes: a multicentre randomised crossover trial, Lancet 389 (10067) (2017) 369–380.

[3] B.W. Bequette, Challenges and recent progress in the development of a closed-loop artificial pancreas, Annu. Rev. Control 36 (2) (2012) 255–266.

[4] G.M. Steil, A.E. Panteleon, K. Rebrin, Closed-loop insulin delivery-the path to physiological glucose control, Adv. Drug Deliv. Rev. 56 (2) (2004) 125–144.

[5] J. Walsh, R. Roberts, L. Heinemann, Confusion regarding duration of insulin action: a potential source for major insulin dose errors by bolus calculators, J. Diabetes Sci. Technol. 8 (1) (2014) 170–178.

[6] Patricio Colmegna, R.S. Sánchez-Peña, Analysis of three T1DM simulation models for evaluating robust closed-loop controllers, Comput. Methods Programs Biomed. 113 (1) (2014) 371–382.

[7] B.P. Kovatchev, M. Breton, C. Dalla Man, C. Cobelli, In silico model and computer simulation environment approximating the human glucose/insulin utilization, Food and Drug Administration Master File MAF 1521, 2008.

[8] B.P. Kovatchev, M. Breton, C. Dalla Man, C. Cobelli, In silico preclinical trials: a proof of concept in closed-loop control of type 1 diabetes, J. Diabetes Sci. Technol. 3 (1) (2009) 44–55.

[9] R. Hovorka, D. Elleri, H. Thabit, J. Allen, L. Leelarathna, R. El-Khairi, K. Kumareswaran, K. Caldwell, P. Calhoun, C. Kollman, H. Murphy, C. Acerini, M. Wilinska, M. Nodale, D. Dunger, Overnight closed-loop insulin delivery in young people with type 1 diabetes: a free-living, randomized clinical trial, Diabetes Care 37 (5) (2014) 1204–1211.

[10] R. Gondhalekar, E. Dassau, F.J. Doyle III, Periodic zone-MPC with asymmetric costs for outpatient-ready safety of an artificial pancreas to treat type 1 diabetes, Automatica 71 (9) (2016) 237–246.

[11] Moshe Phillip, Tadej Battelino, Eran Atlas, Olga Kordonouri, Natasa Bratina, Shahar Miller, Torben Biester, Magdalena Stefanija, Ido Muller, Revital Nimri, Thomas Danne, Nocturnal glucose control with an artificial pancreas at a diabetes camp, N. Engl. J. Med. 368 (9) (2013) 824–833.

[12] Martin de Bock, Anirban Roy, Matthew Cooper, Julie Dart, Carolyn Berthold, Adam Retterath, Kate Freeman, Benyamin Grosman, Natalie Kurtz, Fran Kaufman, Timothy Jones, Elizabeth Davis, Feasibility of outpatient 24-hour closed-loop insulin delivery, Diabetes Care 38 (11) (2015) e186–e187.

[13] R.S. Sánchez-Peña, P. Colmegna, L. Grosembacher, M. Breton, H. De Battista, F. Garelli, W. Belloso, E. Campos-Náñez, V. Simonovich, V. Beruto, P. Scibona, D. Cherñavvsky, Artificial pancreas: first clinical trials in Argentina, in: 20th IFAC World Congress, Toulouse, France, 2017, pp. 7997–8002.

[14] T.T. Ly, A. Roy, B. Grosman, J. Shin, A. Campbell, S. Monirabbasi, B. Liang, R. von Eyben, S. Shanmugham, P. Clinton, B.A. Buckingham, Day and night closed-loop control using the integrated Medtronic hybrid closed-loop system in type 1 diabetes at diabetes camp, Diabetes Care 38 (7) (2015) 1205–1211.

[15] L. Bally, H. Thabit, H. Kojzar, J.K. Mader, J. Qerimi-Hyseni, S. Hartnell, M. Tauschmann, J.M. Allen, M.E. Wilinska, T.R. Pieber, M.L. Evans, R. Hovorka, Day-and-night glycaemic control with closed-loop insulin delivery versus conventional insulin pump therapy in free-living adults with well controlled type 1 diabetes: an open-label, randomised, crossover study, Lancet Diabetes Endocrinol. 5 (4) (2017) 261–270.

[16] Boris P. Kovatchev, Peiyao Cheng, Stacey M. Anderson, Jordan E. Pinsker, Federico Boscari, Bruce A. Buckingham, Francis J. Doyle III, Korey K. Hood, Sue A. Brown, Marc D. Breton, Daniel Chernavvsky, Wendy C. Bevier, Paige K. Bradley, Daniela Bruttomesso, Simone Del Favero, Roberta Calore, Claudio Cobelli, Angelo Avogaro, Trang T. Ly, Satya Shanmugham, Eyal Dassau, Craig Kollman, John W. Lum, Roy W. Beck, Feasibility of long-term closed-loop control: a multicenter 6-month trial of 24/7 automated insulin delivery, Diabetes Technol. Ther. 19 (1) (2017) 18–24.

[17] G.P. Forlenza, S. Deshpande, T.T. Ly, D.P. Howsmon, F. Cameron, N. Baysal, E. Mauritzen, T. Marcal, L. Towers, B.W. Bequette, L.M. Huyett, J.E. Pinsker, R. Gondhalekar, F.J. Doyle III, D.M. Maahs, B.A. Buckingham, E. Dassau, Application of zone model predictive control artificial pancreas during extended use of infusion set and sensor: a randomized crossover-controlled home-use trial, Diabetes Care 40 (8) (2017) 1096–1102.

[18] Mirko Messori, Jort Kropff, Simone Del Favero, Jerome Place, Roberto Visentin, Roberta Calore, Chiara Toffanin, Federico Di Palma, Giordano Lanzola, Anne Farret, Federico Boscari, Silvia Galasso, Angelo Avogaro, Patrick Keith-Hynes, Boris P. Kovatchev, Daniela Bruttomesso, Lalo Magni, J. Hans DeVries, Eric Renard, Claudio Cobelli, for the AP@home consortium, Individually adaptive artificial pancreas in subjects with type 1 diabetes: a one-month proof-of-concept trial in free-living conditions, Diabetes Technol. Ther. 19 (10) (2017) 560–571.

[19] A. Haidar, V. Messier, L. Legault, M. Ladouceur, R. Rabasa-Lhoret, Outpatient 60-hour day-and-night glucose control with dual-hormone artificial pancreas, single-hormone artificial pancreas, or sensor-augmented pump therapy in adults with type 1 diabetes: an open-label, randomised, crossover, controlled trial, Diabetes Obes. Metab. 19 (5) (2017) 713–720.

[20] Stuart A. Weinzimer, Garry M. Steil, Karena L. Swan, Jim Dziura, Natalie Kurtz, William V. Tamborlane, Fully automated closed-loop insulin delivery versus semiautomated hybrid control in pediatric patients with type 1 diabetes using an artificial pancreas, Diabetes Care 31 (5) (2008) 934–939.

[21] A.S. Brazeau, H. Mircescu, K. Desjardins, C. Leroux, I. Strychar, J.M. Ekoé, R. Rabasa-Lhoret, Carbohydrate counting accuracy and blood glucose variability in adults with type 1 diabetes, Diabetes Res. Clin. Pract. 99 (1) (2013) 19–23.

[22] V. Gingras, R. Rabasa-Lhoret, V. Messier, M. Ladouceur, L. Legault, A. Haidar, Efficacy of dual-hormone artificial pancreas to alleviate the carbohydrate-counting burden of type 1 diabetes: a randomized crossover trial, Diabetes Metab. 42 (1) (2016) 47–54.

[23] V. Gingras, A. Haidar, V. Messier, L. Legault, M. Ladouceur, R. Rabasa-Lhoret, A simplified semi-quantitative meal bolus strategy combined with single- and dual-hormone closed-loop delivery in patients with type 1 diabetes: a pilot study, Diabetes Technol. Ther. 18 (8) (2016) 464–471.

[24] G.M. Steil, K. Rebrin, C. Darwin, F. Hariri, M.F. Saad, Feasibility of automating insulin delivery for the treatment of type 1 diabetes, Diabetes 55 (12) (2006) 3344–3350.
[25] E. Dassau, H. Zisser, R. Harvey, M. Percival, B. Grosman, W. Bevier, E. Atlas, S. Miller, R. Nimri, L. Jovanovič, F.J. Doyle III, Clinical evaluation of a personalized artificial pancreas, Diabetes Care 36 (4) (2013) 801–809.
[26] M. Reddy, P. Herrero, M.E. Sharkawy, P. Pesl, N. Jugnee, D. Pavitt, I.F. Godsland, G. Alberti, C. Toumazou, D.G. Johnston, P. Georgiou, N.S. Oliver, Metabolic control with the bio-inspired artificial pancreas in adults with type 1 diabetes: a 24-hour randomized controlled crossover study, J. Diabetes Sci. Technol. 10 (2) (2015) 405–413.
[27] H. Blauw, A.C. van Bon, R. Koops, J.H. DeVries, on behalf of the PCDIAB consortium, Performance and safety of an integrated bihormonal artificial pancreas for fully automated glucose control at home, Diabetes Obes. Metab. 18 (7) (2016) 671–677.
[28] F.M. Cameron, T.T. Ly, B.A. Buckingham, D.M. Maahs, G.P. Forlenza, C.J. Levy, D. Lam, P. Clinton, L.H. Messer, E. Westfall, C. Levister, Y.Y. Xie, N. Baysal, D. Howsmon, S.D. Patek, B.W. Bequette, Closed-loop control without meal announcement in type 1 diabetes, Diabetes Technol. Ther. 19 (9) (2017) 527–532.
[29] K. Turksoy, I. Hajizadeh, S. Samadi, J. Feng, M. Sevil, M. Park, L. Quinn, E. Littlejohn, A. Cinar, Real-time insulin bolusing for unannounced meals with artificial pancreas, Control Eng. Pract. 59 (Supplement C) (2017) 159–164.
[30] F.M. Cameron, G. Niemeyer, B.W. Bequette, Extended multiple model prediction with application to blood glucose regulation, J. Process Contr. 22 (8) (2012) 1422–1432.
[31] Ali Cinar, Special issue on artificial pancreas systems, IEEE Control Syst. Mag. 38 (1) (2018).
[32] P. Colmegna, R.S. Sánchez-Peña, R. Gondhalekar, E. Dassau, F.J. Doyle III, Reducing risks in type 1 diabetes using $\mathcal{H}_\infty$ control, IEEE Trans. Biomed. Eng. 61 (12) (2014) 2939–2947.
[33] P. Colmegna, R.S. Sánchez-Peña, R. Gondhalekar, E. Dassau, F.J. Doyle III, Switched LPV glucose control in type 1 diabetes, IEEE Trans. Biomed. Eng. 63 (6) (2016) 1192–1200.
[34] P. Colmegna, R.S. Sánchez-Peña, R. Gondhalekar, E. Dassau, F.J. Doyle III, Reducing glucose variability due to meals and postprandial exercise in T1DM using switched LPV control: in silico studies, J. Diabetes Sci. Technol. 10 (3) (2016) 744–753.
[35] P. Colmegna, F. Garelli, H. De Battista, Ricardo Sánchez-Peña, Automatic regulatory control in type 1 diabetes without carbohydrate counting, Control Eng. Pract. 74 (2018) 22–32.
[36] A. Revert, F. Garelli, J. Picó, H. De Battista, P. Rossetti, J. Vehi, J. Bondía, Safety auxiliary feedback element for the artificial pancreas in type 1 diabetes, IEEE Trans. Biomed. Eng. 60 (8) (2013) 2113–2122.
[37] F. León-Vargas, F. Garelli, H. De Battista, J. Vehi, Postprandial response improvement via safety layer in closed-loop blood glucose controllers, Biomed. Signal Process. Control 16 (2015) 80–87.
[38] R.A. Gómez-Díaz, N. Garibay-Nieto, N. Wacher-Rodarte, C.A. Aguilar-Salinas, Epidemiology of type 1 diabetes in Latin America, Curr. Diabetes Rev. 10 (2) (2014) 75–85.
[39] J.E. Caporale, J.F. Elgart, J.J. Gagliardino, Diabetes in Argentina: cost and management of diabetes and its complications and challenges for health policy, Glob. Health 9 (54) (2013).
[40] L. González, J.E. Caporale, J.F. Elgart, J.J. Gagliardino, The burden of diabetes in Argentina, Glob. J. Health Sci. 7 (3) (2015) 124–133.
[41] R.S. Sánchez-Peña, F.D. Bianchi, Model selection: from LTI to switched-LPV, in: American Control Conference, ACC, Montreal, Canada, 2012, pp. 1561–1566.
[42] Stephen D. Patek, B. Wayne Bequette, Marc Breton, Bruce A. Buckingham, Eyal Dassau, Francis J. Doyle III, John Lum, Lalo Magni, Howard C. Zisser, In silico preclinical trials: methodology and engineering guide to closed-loop control in type 1 diabetes mellitus, J. Diabetes Sci. Technol. 3 (2) (2009) 269–282.
[43] P.G. Fabietti, V. Canonico, M.O. Federici, M.M. Benedetti, E. Sarti, Control oriented model of insulin and glucose dynamics in type 1 diabetics, Med. Biol. Eng. Comput. 44 (1–2) (2006) 69–78.
[44] S. Schaller, S. Willmann, J. Lippert, L. Schaupp, T.R. Pieber, A. Schuppert, T. Eissing, A generic integrated physiologically based whole-body model of the glucose-insulin-glucagon regulatory system, CPT: Pharmacometrics Syst. Pharmacol. 2 (8) (2013) 1–10, https://doi.org/10.1038/psp.2013.40.

[45] S.S. Kanderian, S.A. Weinzimer, G.M. Steil, The identifiable virtual patient model: comparison of simulation and clinical closed-loop study results, J. Diabetes Sci. Technol. 6 (2) (2012) 371–379.

[46] Q. Wang, P. Molenaar, S. Harsh, K. Freeman, J. Xie, C. Gold, M. Rovine, J. Ulbrecht, Personalized state-space modeling of glucose dynamics for type 1 diabetes using continuously monitored glucose, insulin dose, and meal intake: an extended Kalman filter approach, J. Diabetes Sci. Technol. 8 (2) (2014) 331–345.

[47] J. Walsh, R. Roberts, Pumping Insulin, fourth ed., Torrey Pines Press, San Diego, CA, 2006.

[48] Klaske van Heusden, Eyal Dassau, Howard C. Zisser, Dale E. Seborg, Francis J. Doyle III, Control-relevant models for glucose control using a priori patient characteristics, IEEE Trans. Biomed. Eng. 59 (7) (2012) 1839–1849.

[49] J.B. Lee, E. Dassau, D.E. Seborg, F.J. Doyle III, Model-based personalization scheme of an artificial pancreas for type 1 diabetes applications, in: American Control Conference, ACC, Washington, DC, USA, 2013, pp. 2911–2916.

[50] R. Gondhalekar, E. Dassau, H.C. Zisser, F.J. Doyle III, Periodic-zone model predictive control for diurnal closed-loop operation of an artificial pancreas, J. Diabetes Sci. Technol. 7 (6) (2013) 1446–1460.

[51] Y.C. Kudva, R.E. Carter, C. Cobelli, R. Basu, A. Basu, Closed-loop artificial pancreas systems: physiological input to enhance next-generation devices, Diabetes Care 37 (5) (2014) 1184–1190.

[52] F.J. Doyle III, L.M. Huyett, J.B. Lee, H.C. Zisser, E. Dassau, Closed-loop artificial pancreas systems: engineering the algorithms, Diabetes Care 37 (5) (2014) 1191–1197.

[53] L. Kovács, B. Kulcsár, J. Bokor, Z. Benyó, LPV fault detection of glucose-insulin system, in: 14th Mediterranean Conference on Control and Automation, Ancona, Italy, 2006, pp. 1–5.

[54] R.S. Sánchez-Peña, A.S. Ghersin, LPV control of glucose for diabetes type I, in: 32nd Annual International Conference, Buenos Aires, Argentina, IEEE EMBS, 2010, pp. 680–683.

[55] L. Kovács, B. Kulcsár, LPV modeling of type I diabetes mellitus, in: 8th International Symposium of Hungarian Researchers, Budapest, Hungary, 2007, pp. 163–173.

[56] L. Kovács, B. Kulcsár, J. Bokor, Z. Benyó, Model-based nonlinear optimal blood glucose control of type I diabetes patients, in: 30th Annual International IEEE EMBS Conference, Vancouver, BC, Canada, 2008, pp. 1607–1610.

[57] L. Kovács, B. Benyó, J. Bokor, Z. Benyó, Induced $\mathcal{L}_2$-norm minimization of glucose–insulin system for type I diabetic patients, Comput. Methods Programs Biomed. 102 (2) (2011) 105–118.

[58] P. Szalay, G. Eigner, L.A. Kovács, Linear matrix inequality-based robust controller design for type-1 diabetes model, in: 19th IFAC World Congress, Cape Town, South Africa, 2014, pp. 9247–9252.

[59] R.N. Bergman, Y. Ider, C. Bowden, C. Cobelli, Quantitative estimation of insulin sensitivity, Am. J. Physiol. 236 (6) (1979) E667–E677.

[60] J.T. Sorensen, A Physiologic Model of Glucose Metabolism in Man and Its Use to Design and Asses Improved Insulin Therapies for Diabetes, Ph.D. thesis, Massachusetts Institute of Technology, Cambridge, MA, USA, 1985.

[61] R. Hovorka, F. Shojaee-Moradie, P.V. Carroll, L.J. Chassin, I.J. Gowrie, N.C. Jackson, R.S. Tudor, A.M. Umpleby, R.H. Jones, Partitioning glucose distribution/transport, disposal, and endogenous production during IVGTT, Am. J. Physiol. Endocrinol. Metab. 282 (5) (2002) E992–E1007.

[62] P. Colmegna, R. Sánchez-Peña, R. Gondhalekar, Control-oriented linear parameter-varying model for glucose control in type 1 diabetes, in: IEEE Multi-Conference on Systems and Control, Buenos Aires, Argentina, 2016, pp. 410–415.

[63] P. Colmegna, R. Sánchez-Peña, R. Gondhalekar, Linear parameter-varying model to design control laws for an artificial pancreas, Biomed. Signal Process. Control 40 (2018) 204–213.

[64] B.P. Kovatchev, M. Breton, C. Dalla Man, C. Cobelli, In silico preclinical trials: a proof of concept in closed-loop control of type 1 diabetes, J. Diabetes Sci. Technol. 3 (1) (2009) 44–55.

[65] C. Dalla Man, F. Micheletto, D. Lv, M. Breton, B.P. Kovatchev, C. Cobelli, The UVA/PADOVA type 1 diabetes simulator: new features, J. Diabetes Sci. Technol. 8 (1) (2014) 26–34.

[66] G. Vinnicombe, Frequency domain uncertainty and the graph topology, IEEE Trans. Autom. Control 38 (9) (1993) 1371–1383.

[67] G. Vinnicombe, Uncertainty and Feedback: $\mathcal{H}_\infty$ Loop-Shaping and the ν-Gap Metric, Imperial College Press, London, 2001.
[68] K.R. Popper, Conjectures and Refutations: The Growth of Scientific Knowledge, Routledge, London, 1963.
[69] F. Bianchi, M. Moscoso-Vázquez, P. Colmegna, R. Sánchez-Peña, Invalidation and low-order model set for artificial pancreas robust control design, J. Process Control (2019), https://doi.org/10.1016/j.jprocont.2019.02.004, in press.
[70] Roy S.R. Smith, Model Validation for Uncertain Systems, Ph.D. thesis, California Institute of Technology, 1990.
[71] Mario Sznaier, María C. Mazzaro, An LMI approach to control-oriented identification and model (in)validation of LPV systems, IEEE Trans. Autom. Control 48 (9) (2003) 1619–1624.
[72] R. Smith, G. Dullerud, S. Rangan, K. Poolla, Model validation for dynamically uncertain systems, Math. Comput. Model. Dyn. Syst. 3 (1) (1997) 43–58.
[73] J.P. Hespanha, A.S. Morse, Switching between stabilizing controllers, Automatica 38 (11) (2002) 1905–1917.
[74] F. Garelli, R. Mantz, H. De Battista, Advanced Control for Constrained Processes and Systems, IET Institution of Engineering and Technology, London, United Kingdom, 2011.
[75] M.E. Willinska, L.J. Chassin, H.C. Schaller, L. Schaupp, T.R. Pieber, R. Hovorka, Insulin kinetics in type 1 diabetes: continuous and bolus delivery of rapid acting insulin, IEEE Trans. Biomed. Eng. 52 (1) (2005) 3–12.
[76] Fabián M.L. Vargas, Design and Implementation of a Closed-Loop Blood Glucose Control Systems in Patients with Type 1 Diabetes, Ph.D. thesis, Universitat de Girona, 2013.
[77] B. Kovatchev, G. Umpierrez, A. DiGenio, R. Zhou, S.E. Inzucchi, Sensitivity of traditional and risk-based glycemic variability measures to the effect of glucose-lowering treatment in type 2 diabetes mellitus, J. Diabetes Sci. Technol. 9 (6) (2015) 1227–1235.
[78] P. Keith-Hynes, B. Mize, A. Robert, J. Place, The diabetes assistant: a smartphone-based system for real-time control of blood glucose, Electronics 3 (4) (2014) 609–623.